X-ray Diffraction Study of the Electronic Ground State of (*meso*-Tetraphenylporphinato)iron(II)

Naiyin Li,[†] Zhengwei Su,[†] Philip Coppens,*[,†] and John Landrum[‡]

Contribution from the Chemistry Department, State University of New York at Buffalo, Buffalo, New York 14214, and the Department of Chemistry, Florida International University, Miami, Florida 33199. *Received March 5, 1990*

Abstract: The charge distribution in crystalline (*meso*-tetraphenylporphinato)iron(II) has been derived from 10 154 intensity data measured at 120 (5) K. Crystal data are a = 14.992 (2) Å, c = 13.778 Å, Z = 4, space group $I\bar{4}2d$. The data have been analyzed with the aspherical-atom multipole formalism including anharmonic thermal parameters for the iron atom. The deformation density maps indicate preferential occupancy of the d_{z^2} and d_{xy} orbitals of the iron atom, a conclusion confirmed by the d-orbital populations derived from the aspherical-atom multipole refinement. The results are in agreement with an SCF-CI calculation by Rohmer[1] and an INDO-CI calculation by Edwards, Weiner, and Zerner[2] and support the $^3A_{2g}$ state as the leading contributor to the ground state of the complex. The ground-state assignment is in contrast to results on the intermediate spin complex iron(II) phthalocyanine, for which the electron density indicates a ^3E_g ground state.[3] The difference is attributed to the effect of short intermolecular Fe-N contacts in crystalline iron(II) phthalocyanine on the relative order of closely spaced energy levels.

Introduction

The nature of the electronic ground state of the four-coordinate iron(II) porphyrins and phthalocyanins has been the subject of considerable controversy. While the complexes are generally agreed to be in an intermediate spin state, conclusions about the correct assignment of the term symbols vary. Most recent studies of iron(II) porphyrin (FeP) agree that the $^3A_{2g}[(d_{xy})^2(d_{xz,yz})^2(d_{z^2})^2]$ and the $^3E_g[(d_{xy})^2(d_{xz,yz})^3(d_{z^2})^1]$ states are low lying and separated by an energy that is typically estimated to be 200–2000 cm^{-1}. The ambiguity in the theoretical treatments is related to the existence of a number of closely spaced electronic states. Conclusions regarding the nature of the ground state depend on the details of the calculation, and in particular on the treatment of electron correlation.[2] In some calculations the relative ordering is inversed when electron correlation is taken into account.[4]

As the measured magnetic moments of iron(II) (mesotetraphenyl)porphyrin (FeTPP) [4.2,[5] 4.4,[6] and 4.75 μB[7]] are quite different from the spin-only value of 2.8 μB, there is a considerable orbital contribution. Consequently, various states are expected to mix through spin–orbit coupling, and the ground state is likely to be a mixture of several SCF configurations, which further complicates the assignment.

While many experimental techniques cannot distinguish between the $^3A_{2g}$ and ^3E_g states (for example the UV spectra are calculated to be similar, while Mossbauer quadrupole splittings are inconclusive, and NMR and resonance Raman studies lead to opposing conclusions[2]), there are marked differences in the distribution of the iron valence electrons over the d-orbitals. Thus, the corresponding electron distributions will be distinct, as illustrated by recent SCF-CI results.[1] It is therefore reasonable to expect that a distinction between leading contributors to the ground-state configuration can be made on the basis of the experimentally determined electron distribution.

The present study is a continuation of charge density analyses of a number of iron porphyrins and phthalocyanins of differing coordination, valency, and spin state. For iron(II) phthalocyanine (FePc) both the experimental electron density and the d-orbital populations derived from the diffraction data clearly indicate the ^3E_g state to be the leading contributor to the ground state of the molecule.[3] Other iron(II) complexes of which the electron density has been determined include bis(tetrahydrofuran)(*meso*-tetraphenylporphinato)iron(II),[8] and bis(pyridine)(*meso*-tetraphenylporphinato)iron(II) (Fe(py)$_2$TPP).[9]

A previous analysis of FeTPP was ambiguous due to difficulties encountered during the data collection but seemed to indicate that the ^3E_g state was not the main contributor to the molecular ground state.[10] In the new study reported here great care was taken to avoid interruption of the data collection, and a much smaller crystal was used. The agreement between symmetry equivalent reflections and the low noise level in the resulting maps attest to the quality of the experimental data.

It should be noted that the X-ray results apply to the molecule embedded in its crystal matrix and not to the isolated species. Calculations on "basket-handle" porphyrins have shown that small perturbations caused by axial benzene rings at about 3 Å from

Table I. Experimental Details

formula	$FeN_4C_{44}H_{28}$
mol wt	668.59
space group	$I\bar{4}2d$
Z	4
exptl temp, K	120 (5)
cryst dimens, mm	0.25 × 0.23 × 0.25
cell dimens, Å	a = 14.992 (2) c = 13.778 (2)
unit cell vol, Å^3	3096.7
d(calc), g cm^{-3}	1.434
X-ray wavelength, Å	0.71069
abs coeff, cm^{-1}	5.24
scan mode	θ–2θ step scan
scan width	1.0 + 0.525 tan θ
$(\sin\theta/\lambda)_{max}$, Å^{-1}	1.23
no. of reflcns collected	10154
no. of unique reflcns	2786
no. of reflcns with $I > 2.0\sigma(I)$	2018
no. of reflcns with $I > 1.5\sigma(I)$	2284

[†] State University of New York at Buffalo.
[‡] Florida International University.

(1) Rohmer, M. M. *Chem. Phys. Lett.* **1985**, *116*, 44–49.
(2) Edwards, W. D.; Weiner, B.; Zerner, M. C. *J. Am. Chem. Soc.* **1986**, *108*, 2196–2204.
(3) Coppens, P.; Li, L. *J. Chem. Phys.* **1984**, *81*, 1983–1993.
(4) Rawlings, D. C.; Gouterman, M.; Davidson, E. R.; Feller, D. *Int. J. Quantum Chem.* **1985**, *XXVIII*, 773–796.
(5) Kobayashi, H.; Yanagawa, Y. *Bull. Chem. Soc. Jpn.* **1972**, *45*, 450–456.
(6) Collman, J. P.; Hoard, J. L.; Kim, N.; Lang, G.; Reed, C. A. *J. Am. Chem. Soc.* **1975**, *97*, 2676–2681.
(7) Boyd, P. S. W.; Buckingham, D. A.; McMeeking, R. F.; Mitra, S. *Inorg. Chem.* **1979**, *18*, 3585–3591.
(8) Lecomte, C.; Blessing, R. H.; Coppens, P.; Tabard, A. *J. Am. Chem. Soc.* **1986**, *108*, 6942–6950.
(9) Li, N.; Coppens, P.; Landrum, J. *Inorg. Chem.* **1988**, *27*, 482–488. Mallinson, P. R.; Koritsanszky, T.; Eklaim, E.; Li, N.; Coppens, P. *Acta Crystallogr.* **1988**, *A44*, 336–343.
(10) Tanaka, K.; Elkaim, E.; Liang, L.; Jue, Z. N.; Coppens, P.; Landrum, J. *J. Chem. Phys.* **1986**, *84*, 6969–6978.

0002-7863/90/1512-7294$02.50/0

Table II. Summary of Least-Squares Refinement

	free atom refinement		multipole refinement		
	harmonic	anharmonic Fe	harmonic	anharmonic Fe	anharmonic Fe including 4s
reflections included	$I \geq 2\sigma(I)$	$I \geq 2\sigma(I)$	$I \geq 1.5\sigma(I)$	$I \geq 1.5\sigma(I)$	$I \geq 1.5\sigma(I)$
refine on	F			F	
N_{obs}	2018	2018	2284	2284	2279
N_{var}	137[a]	137[b]	210[c]	215[d]	216[e]
R(F)	0.0469	0.0421	0.0379	0.0377	0.0363
R_w(F)	0.0312	0.0281	0.0203	0.0203	0.0192
G.O.F.	1.049	0.9463	0.6525	0.6535	0.6169

[a] Scale factor, x, y, z, U_{ij} (non-H atoms), U_{iso} (H atoms) are refined. [b] Same as in *a*, plus 5 anharmonic temperature factors of Fe atoms, U_{iso} for H atoms kept constant. [c] Same as in *a*, plus κ, κ', valence population parameters, and multipole coefficients. [d] Same as in *c*, plus 5 anharmonic temperature factors of Fe atoms. [e] Same as in *d*, plus 1 4s population parameter of Fe atom.

the Fe can invert the ordering of the ^3E_g and $^3A_{2g}$ energy levels.[11] Thus the nature of the ground state may be affected by crystal packing effects, as is indeed suggested by the comparison of the present results with those obtained earlier on iron(II) phthalocyanine.

Experimental Section

Sample Preparation. All synthetic steps, including solvent purification, were carried out in a Vacuum/Atmospheres glovebox. Solvents were AR grade and prepared by drying over $CaCl_2$ (benzene and heptane) and distilled from Na/benzophenone (benzene only) or degassed by bubbling (ethanol, gold label) and were stored sealed inside the glovebox prior to use. FeTPP was prepared by reduction of Fe^{III}(TPP)Cl by the method of Collman et al[12] with $Cr(acac)_2$. Suitable single crystals of the desired dimensions were obtained by direct crystallization of FeTPP from the reaction medium upon slow addition of ethanol followed by heptane.

Data Collection. An approximately octahedral, purple-colored crystal of dimensions 0.25 × 0.23 × 0.25 mm was sealed in a capillary in a nitrogen atmosphere. Unit cell dimensions were obtained by least-squares refinement of 25 reflections with $20 < \theta < 32°$. Data were collected at 120 (5) K on a Nonius CAD-4 diffractometer, using a gas-flow cooling device. Data collection details are summarized in Table I. Four standard reflections measured at regular intervals showed a maximal decrease of 1% in intensity during data collection.

Data Reduction. The reflection profiles were analyzed with a program by Blessing,[13] based on the Lehmann–Larsen formalism.[14] Averaging of symmetry equivalent reflections gave 2786 unique reflections, of which 2018 and 2284 have intensities larger than $2\sigma(I)$ and $1.5\sigma(I)$, respectively. The internal agreement factor between the intensities of symmetry-equivalent reflections was 2.4%.

Refinements. In all least-squares refinements the function $\sum w(F_o - k|F_c|)^2$ was minimized. The weights w are defined by $w(F) = 1/\sigma^2(F_{obs}) = 4F^2/\sigma^2(F^2)$, with $\sigma^2(F^2) = pF^2 + \sigma^2_{counting}(F^2)$. The factor p was based on the fluctuation of the standard reflections. Values of 0.007 and 0.011 were used for different parts of the data set.

Four different refinements were performed: (1) a conventional spherical atom refinement; (2) a multipole refinement in which the atomic density is described by the sum of a core density, a spherical valence density with adjustable population $P_{valence}$, and radial parameter κ, and a set of atomic deformation terms with variable population P_{lmp} and radial parameter κ', according to the expression[15,16]

$$\rho_{atom}(r) = \rho_{core}(r) + \kappa^3 P_{valence}\rho_{valence}(\kappa r) + \kappa'^3 \sum_l \sum_m \sum_p P_{lmp} R_l(\kappa' r) y_{lmp}(\theta,\phi) \quad (1)$$

where y_{lmp} are the real spherical harmonic functions with $p = \pm$, and R_l is a radial function; (3) a multipole refinement with anharmonic thermal parameters on the iron atoms according to the Gram–Charlier formalism;[17,18] and (4) refinement 3 with an additional spherical function on the iron atom representing the 4s density.

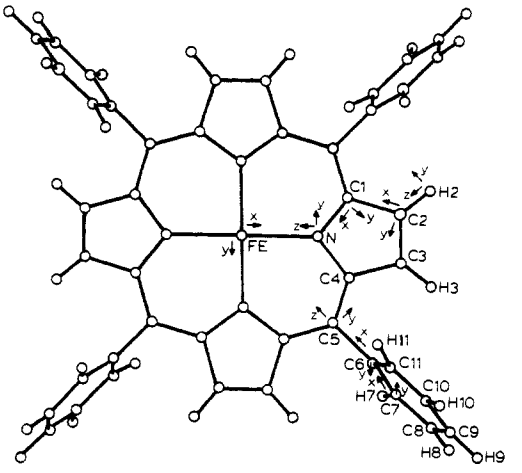

Figure 1. Labeling of the atoms and definition of local coordinate systems.

Table III. Positional and Equivalent Isotropic Thermal Parameters[a]

atom	x	y	z	B_{equi},[b] Å^2
Fe	0.000	0.000	0.000	0.826 (7)
N	0.1134 (1)	0.06580 (9)	−0.0025 (1)	1.11 (3)
C(1)	0.1973 (1)	0.0329 (1)	0.0166 (1)	1.21 (3)
C(2)	0.2623 (1)	0.1035 (1)	0.0161 (1)	1.61 (3)
C(3)	0.2175 (1)	0.1798 (1)	−0.0072 (1)	1.59 (3)
C(4)	0.1249 (1)	0.1561 (1)	−0.0168 (1)	1.19 (3)
C(5)	0.0569 (1)	0.2183 (2)	−0.0300 (1)	1.17 (3)
C(6)	0.0822 (1)	0.3116 (1)	−0.0556 (1)	1.20 (3)
C(7)	0.1047 (1)	0.3324 (1)	−0.1516 (1)	1.58 (3)
C(8)	0.1300 (1)	0.4189 (1)	−0.1766 (1)	1.95 (3)
C(9)	0.1330 (1)	0.4852 (1)	−0.1058 (1)	1.75 (3)
C(10)	0.1105 (1)	0.4652 (1)	−0.0107 (1)	1.92 (3)
C(11)	0.0850 (1)	0.3786 (1)	0.0145 (1)	1.88 (3)
H(2)	0.330 (2)	0.094 (1)	0.029 (1)	4.1 (6)*
H(3)	0.241 (2)	0.244 (2)	−0.016 (1)	4.6 (6)*
H(7)	0.103 (1)	0.282 (2)	−0.203 (2)	5.3 (6)*
H(8)	0.145 (1)	0.434 (1)	−0.248 (3)	6.0 (6)*
H(9)	0.152 (1)	0.550 (2)	−0.124 (1)	4.3 (6)*
H(10)	0.112 (1)	0.515 (2)	0.043 (2)	5.0 (5)*
H(11)	0.069 (1)	0.362 (1)	0.087 (3)	6.3 (6)*

[a] From final multipole refinement without 4s electrons. [b] Starred atoms refined isotropically. Isotropic equivalent thermal parameters defined as: $B = (4/3)[a^2B(1,1) + b^2B(2,2) + c^2B(3,3) + ab(\cos\gamma)\cdot B(1,2) + ac(\cos\beta)B(1,3) + bc(\cos\alpha)B(2,3)]$.

For the C, N, and Fe atoms, scattering factors for the conventional refinements were taken from the *International Tables for X-ray Crystallography*, Vol. 4,[19] while those for the hydrogen atoms were as given by Stewart, Davidson, and Simpson.[20] In the multipole refinement core and spherical valence shell scattering factors are as listed in the *International Tables for X-ray Crystallography*.[19] The radial parts of the

(11) Mispelter, J.; Momenteau, M.; Lhoste, J. M. *J. Chem. Phys.* **1980**, *72*, 1003–1012.
(12) Collman, J. P.; Hoard, J. L.; Kim, N.; Lang, G.; Reed, C. A. *J. Am. Chem. Soc.* **1975**, *97*, 2676–2681.
(13) Blessing, R. H. *Cryst. Rev.* **1987**, *1*, 3–58.
(14) Lehmann, M. S.; Larsen, F. K. *Acta Crystallogr.* **1974**, *A30*, 580–584.
(15) Coppens, P.; Guru Row, T. N.; Leung, P.; Becker, P. J.; Yang, Y. W.; Stevens, E. D. *Acta Crystallogr.* **1979**, *A35*, 63–72.
(16) Hansen, N. K.; Coppens, P. *Acta Crystallogr.* **1978**, *A34*, 909–921.
(17) Zucker, U. H.; Schulz, H. *Acta Crystallogr.* **1982**, *A38*, 568–576.
(18) Mallinson, P. R.; Koritsanszky, T.; Elkaim, E.; Li, N.; Coppens, P. *Acta Crystallogr.* **1988**, *A44*, 336–343.
(19) *International Tables for X-ray Crystallography*; Birmingham: Kynoch Press (present distributor Kluwer Academic Publishers: Dordrecht), 1974; Vol. IV.
(20) Stewart, R. F.; Davidson, E. R.; Simpson, W. T. *J. Chem. Phys.* **1965**, *42*, 3175–3187.

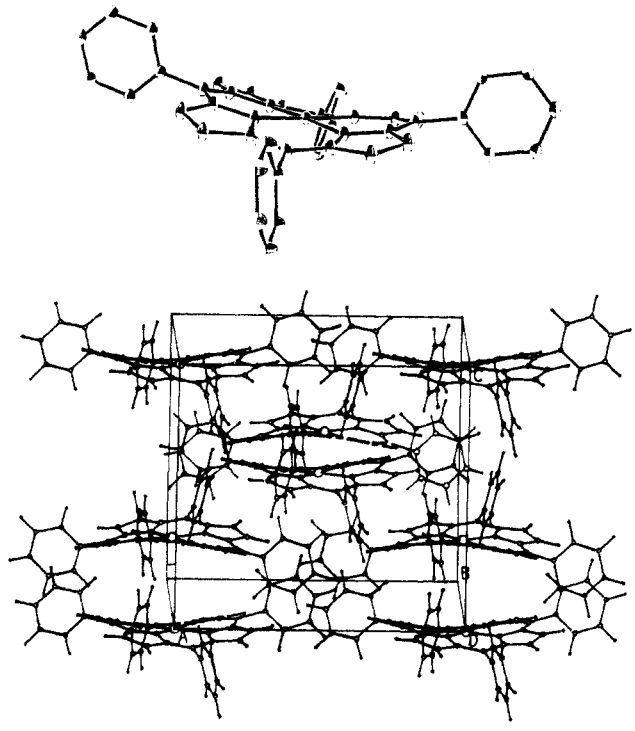

Figure 2. (a) Molecular structure. Ellipsoids are 50% probability surfaces. H atoms are not shown. (b) Packing diagram.

light-atom deformation function were described by Slater-type exponential functions; starting values of the exponential coefficients were as given by Clementi and Raimondi.[21] For the iron atom a κ-modified atomic Hartree–Fock radial function was used for all deformation functions. The local Cartesian coordinate systems, in which the multipole functions are defined, are shown in Figure 1. To reduce the number of charge density parameters, the populations of chemically equivalent atoms were constrained to be equal, and local mirror planes were assumed perpendicular to the porphyrin ring and through the phenyl ring. The resulting local symmetry is as follows: Fe, D_{4h} ($4/mmm$); N atoms, C_{2v} ($mm2$); C atoms, C_s (m). The multipole expansion was truncated at the hexadecapolar level ($l = 4$) for iron, the octapolar level ($l = 3$) for C and N, and the dipolar level ($l = 1$) for the H atoms. As the iron atom site has local centrosymmetric point group symmetry, the anharmonic temperature parameter refinements did not converge when the symmetry-allowed, but center-of-symmetry forbidden third order coefficients C_{113} and C_{123} were included. These parameters were subsequently fixed to zero values. The largest values of the anharmonic temperature parameters are about 3σ (for D_{1111}, D_{3333}, D_{1133}, and D_{2233}, Table S-I, supplementary material) and thus barely significant. The refinements are summarized in Table II, while atomic and charge density parameters are listed in Tables III and S-I and S-II (supplementary material).

The configuration of the molecule and the packing diagram are given in Figure 2. The residual density maps, calculated after the final multipole refinement, are shown in Figure 3. The lack of features in the map indicates that the electron density is well fitted by the refinement. Bond lengths and angles are summarized in Figure 4 and listed in Table S-III (supplementary material).

Deformation Electron Density Maps

Because of the acentric space group the calculation of the deformation density maps requires knowledge of the phases of the reflections.[22] The appropriate expression is given by

$$\Delta\rho = \frac{2}{V}\sum_{\mathbf{h}}^{1/2}\{(A_1 - A_2)\cos(2\pi\mathbf{h}\cdot\mathbf{r}) + (B_1 - B_2)\sin(2\pi\mathbf{h}\cdot\mathbf{r})\} \quad (2)$$

where A_1 and B_1 are $F_{obs}\cos\phi_{multipole}$ and $F_{obs}\sin\phi_{multipole}$, respectively, and $\phi_{multipole}$ is the phase ($\tan^{-1} B/A$) as calculated from the multipole refinement results. A_2 and B_2 are obtained in an analogous manner from the structure factors F and phases ϕ, as calculated from the final model positional and thermal parameters and the spherical atom scattering factors.

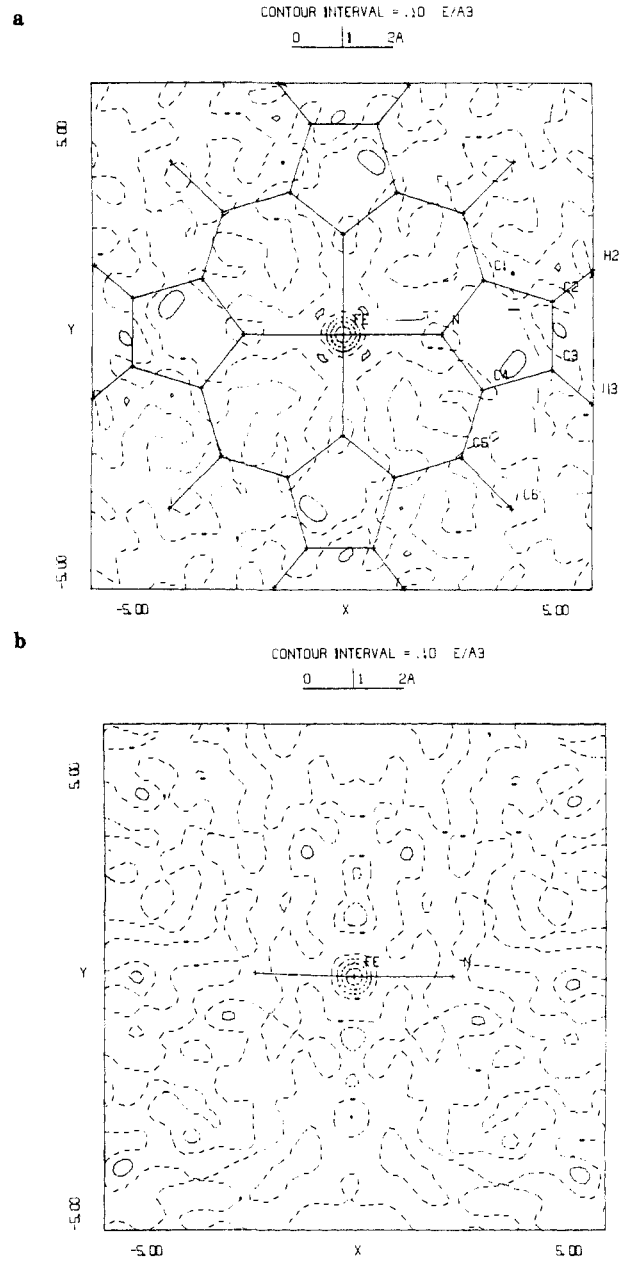

Figure 3. Residual map through the mean porphinato plane calculated with the parameters of the final multipole refinement: (a) in the mean porphinato plane; (b) in the section perpendicular to the porphinato plane containing two pyrrole nitrogen atoms. Contours at 0.1 e Å^{-3}. Zero and negative contours broken.

Deformation density maps in the mean porphinato plane and in a perpendicular plane containing two pyrrole nitrogen atoms are shown in Figure 5. The map through the molecular plane prominently shows the asymmetric features around the iron atom. Lone pair peaks at the nitrogen atoms and density accumulation in all C–C, C–N, and C–H bonds are also evident. As noticed in earlier studies the peaks in the peripheral C–C bonds are more pronounced than those in other C–C bonds, indicating a larger double bond character. The peaks around iron are in the directions diagonal to the Fe–N bonds, as expected for preferential occupancy of the d_{xy} orbital. As shown by Rohmer,[1] this feature is to be expected for both the $^3A_{2g}$ and the ^3E_g states. The two states can be distinguished, however, from the electron density in the z direction from the Fe atom. Here a large peak is observed, as expected for $^3A_{2g}$, but not for ^3E_g, in which the d_{z^2} orbital is populated by only one electron.

This qualitative analysis of the density maps can be placed on a firmer footing by the analysis of the data in terms of the atomic

(21) Clementi, E.; Raimondi, D. L. *J. Chem. Phys.* **1963**, *38*, 2686–2689.
(22) Coppens, P. *Acta Crystallogr.* **1974**, *B30*, 255–261. Becker, P. J.; Coppens, P. *International Tables for X-Ray Crystallography*; Vol. C, in press.

Table IV. Electron Populations on the Iron Atom

	experimental harmonic refinement	theoretical calculations						
		anharmonic Fe	anharmonic Fe with Fe 4s	$^3A_{2g}$(SCF-CI) ref 6	^3E_g(SCF-CI) ref 6	$^3A_{2g}$(INDO-CI) ref 1	^3E_g(INDO-CI) ref 1	^3E_g(EH) ref 31
$d(x^2-y^2)$	0.38 (13) (5.2%)	0.37 (21) (5.4%)	0.46 (21) (7.1%)	0.18 (2.9%)	0.18 (2.9%)	0.487 (7.6%)	0.470 (7.3%)	0.896 (12.8%)
$d(z^2)$	2.31 (12) (31.7%)	2.45 (14) (35.8%)	2.28 (15) (35.0%)	1.94 (31.7%)	0.99 (16.1%)	1.885 (29.5%)	0.985 (15.3%)	1.071 (15.3%)
$d(xz,yz)$	2.81 (16) (38.6%)	2.40 (18) (35.1%)	2.11 (19) (32.4%)	1.98 (32.3%)	2.96 (48.1%)	2.022 (31.7%)	2.988 (46.4%)	3.054 (43.5%)
$d(xy)$	1.79(13) (24.5%)	1.62 (21) (23.7%)	1.66 (21) (25.6%)	2.02 (33.0%)	2.03 (32.8%)	1.992 (31.2%)	1.992 (31.0%)	1.994 (28.4%)
total d	7.28 (27)	6.84 (12)	6.52 (12)	6.12	6.15	6.386	6.435	7.015
4s			1.14 (27)			0.449	0.347	0.349
4p				0.13	0.16	0.422	0.427	0.413

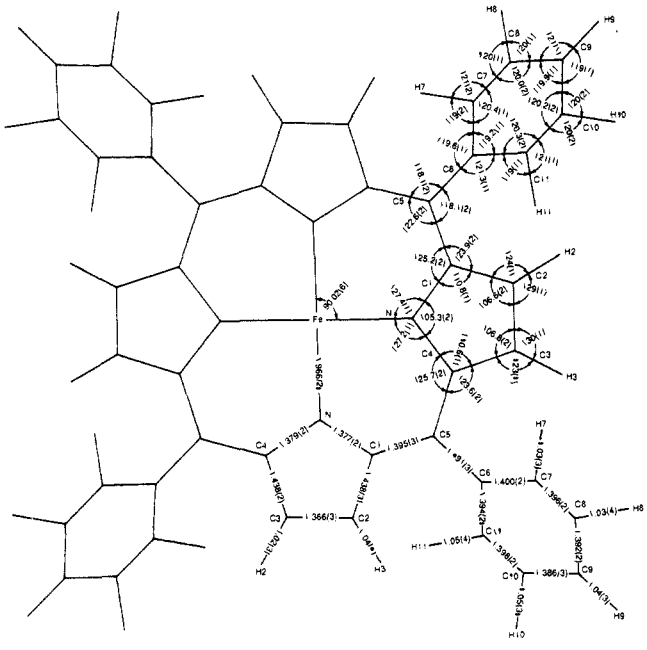

Figure 4. Molecular diagram indicating bond lengths and angles.

multipole expansions, as described in the following section.

Multipole Populations and the d-Electron Distribution

The multipole populations and κ parameters from the aspherical atom refinements are listed in Table S-II (supplementary material). Since the multipoles represent an analytical description of the asphericity of the atomic charge density distribution, the orbital populations of transition metal atoms can, to a good approximation, be derived directly from the multipole populations.[23] The iron valence orbital populations are listed in Table IV, together with the results of a number of theoretical calculations. Differences between the values from the harmonic and anharmonic thermal treatment of the Fe atomic density are not significant, given the experimental standard deviations, and are much smaller than the differences between the theoretical values for the ^3E_g and $^3A_{2g}$ states. The addition of the diffuse 4s density function increases the total charge assigned to the iron atom but has little effect on the aspherical distribution over the iron d-orbitals, a demonstration of the fact that the atomic asphericity is better determined than the net atomic charge, which depends on the partitioning of the overlapping electron density between adjacent atoms.

The experimental d_{z^2} orbital occupancy is not significantly different from 2, and much in excess of the spherical atom population of the Fe(II) atom (1.2 electrons), or the population predicted for the ^3E_g state (1 electron). There is a pleasing agreement between the different theoretical results, except for the population of the $d_{x^2-y^2}$ bonding orbital which shows some discrepancy. The experimental values agree much better with the theoretical results for the $^3A_{2g}$ state, in particular when the percentage occupancies are compared. The final multipole refinement (column 3, anharmonic with 4s) is within the experimental errors equal to the SCF-CI and INDO-CI results for $^3A_{2g}$. The largest discrepancy occurs for the d_{xy} population which tends to be lower according to the experiment. The results are not compatible with the distribution of the ^3E_g state, which differs greatly in the populations of the d_{z^2} and $d_{xz,yz}$ orbitals. It is of interest that the extended Huckel calculation on the ^3E_g state gives a much larger population for the $d_{x^2-y^2}$ bonding orbital than

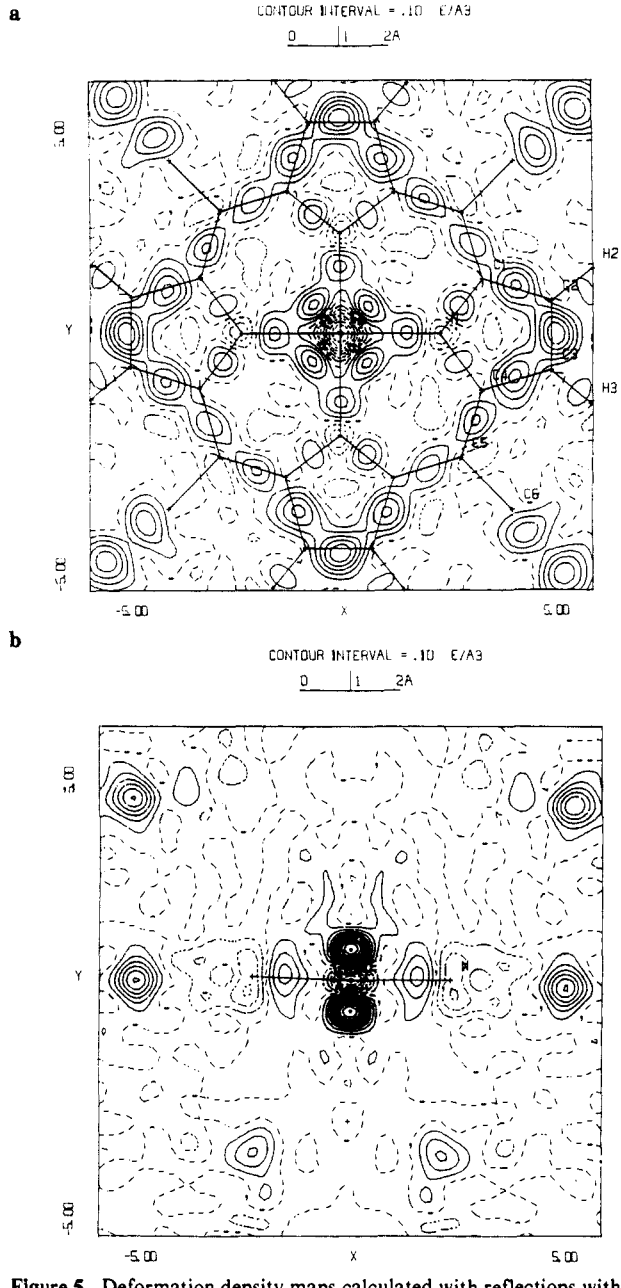

Figure 5. Deformation density maps calculated with reflections with sin $(\theta/\lambda) < 0.7$ Å: (a) in the mean porphinato plane; (b) in the section perpendicular to the porphinato plane containing two pyrrole nitrogen atoms. Contour interval 0.1 e Å^{-3}. Zero and negative contours broken.

(23) Holliday, A.; Leung, P. C.; Coppens, P. *Acta Crystallogr.* **1983**, *A39*, 377–387.

predicted by the SCF theoretical calculation. A similar effect was observed in the comparison of the EH results with the experimental populations on $Fe(py)_2TPP$,[24] even though the other experimental orbital populations agree well with theoretical values for the low-spin singlet ground state of that complex.

Calculation of Quadrupole Splitting Constants

The experimental electron density may be used in the calculation of electrostatic properties, such as the electric field gradient at the iron nucleus, which can also be derived from the quadrupole splitting in Mossbauer spectra. The elements of the electric field gradient tensor contain contributions from the d-electrons, the "valence contribution", as well as the "lattice contribution" due to the net charges and higher multipoles on adjacent atoms. For the tetragonal site of the iron atom in FeTPP the electric field gradient tensor $\nabla\mathbf{E}$ with elements $-\partial^2V/\partial x_i\partial x_j = -V_{ij}$ is described by a single element V_{zz}, to which the other non-zero element V_{xx} ($=V_{yy}$) is related through the zero-trace condition of the tensor.

Expressions for the calculation of the elements of the electric field gradient tensor from the multipole populations have been given by Epstein and Swanton.[25] With the multipole populations of Table S-II from the final refinement (anharmonic treatment of the Fe atom, with 4s contribution) they lead to values of 20 (5) and −0.57 (5) e Å^{-3} for the valence and lattice contributions to ∇E_{zz}, respectively. The latter value is almost completely due to the proximal nitrogen atoms and contains a contribution from the spherical components (−0.49 (3) e Å^{-3}) and the higher order multipole deformation terms (−0.08 (4) e Å^{-3}).

Since the electron density is known with limited resolution, it is appropriate to apply the Sternheimer shielding and antishielding factors in the comparison of the X-ray electric field gradients with the spectroscopic information. The shielding factors are defined by the expression for $eq_{ij} = V_{ij}$:[26]

$$eq_{ij}^{\text{total}} = (1 - R)eq_{ij}^{\text{val}} + (1 - \gamma_\infty)eq_{ij}^{\text{lat}}$$

Typical values of $R = 0.07$ and $\gamma_\infty = -9.1$[27] imply that the valence contribution is shielded and the lattice contribution considerably enhanced. The quadrupole splitting ΔE_{QS} may be obtained with the expression

$$\Delta E_{QS} = \tfrac{1}{2}e^2q_{zz}Q(1 + \eta)^{1/2}$$

where Q is the nuclear quadrupole moment, the asymmetry parameter η being equal to 0 for the tetragonal iron site. Use of $Q = 0.15 \times 10^{-24}$ cm^2 leads to a value of −3.4 (1.1) mm/s, compared with spectroscopic values of ±1.32 and +1.52 mm/s.[28,29] The corresponding value from the harmonic temperature parameter treatment (column 1 of Table S-II) is −2.9 (1.0) mm/s.

We note that the discrepancy in sign between the spectroscopic and crystallographic values is similar to the discrepancy between the spectroscopic value and the splitting based on the $^3A_{2g}$ model derived in the original publication,[29] which the authors attributed to uncertainties in the Sternheimer factors. However, it appears that the discrepancy is too large to be accounted for by adjusting the Sternheimer factor within reasonable limits.

Further Discussion

The most remarkable result of this study is the conclusion that the ground states of the two four-coordinate complexes FePc and FeTPP are different in the crystalline state. There are two obvious differences between the iron environment in the two complexes. The first is intramolecular, the Fe–N distances being shorter in FePc (1.928 (1) Å) than in FeTPP (1.966 (2) Å). The second difference is a result of the large variation in the packing of the molecules in the crystal. In the monoclinic structure of FePc, the porphinato plane is inclined with respect to the Fe–Fe stacking axis, in a way which brings two nitrogen atoms of *b*-axis translation related molecules to a distance of 3.42 Å from the iron atom. The coordination can be described as *pseudo*-6-fold, with the two nitrogen atoms occupying the distant axial positions. In tetragonal FeTPP the molecules are aligned perpendicular to the $\bar{4}$ axis of the space group $I\bar{4}2d$, the closest approach to the iron atom being larger than 6 Å. Given the known sensitivity of the ground-state configuration to axial ligation,[11] it appears that the ground state of FePc is affected by intermolecular interactions. This interpretation suggests that the isolated molecule of FePc would also have $^3A_{2g}$ as the leading contributor, and further that the ground state in solution can be a function of the strength of solvatation. This is in full agreement with known variation in electronic configuration as a function of coordination. For example, while six-coordinate $Fe^{II}(py)_2TPP$ has a low-spin ground state, substitution of the axial ligand by more weakly coordinating THF leads to a high-spin state. The exact nature of the ground states of other analogues of FeTPP, such as monoclinic FeOEP, iron(II) octaethylporphyrin, and orthorhombic FeOEC, iron(II) octaethylchlorin,[30] remain subjects for further study.

Acknowledgment. Support of this work by the National Institutes of Health (5RO1HL2388409) and the National Science Foundation (CHE8711736) is gratefully acknowledged.

Supplementary Material Available: A listing of anisotropic temperature parameters, multipole population of FeTPP, bond distances, and bond angles (6 pages); tables of structure factors (14 pages). Ordering informationis given on any current masthead page.

(24) Li, N.; Coppens, P.; Landrum, J. *Inorg. Chem.* **1988**, *27*, 482–488.
(25) Epstein, J.; Swanton, D. J. *J. Chem. Phys.* **1982**, *77*, 1048–1060.
(26) Sternheimer, R. M.; Foley, H. M. *Phys. Rev.* **1956**, *102*, 731–732.
(27) Ray, S. N.; Das, T. P. *Phys. Rev.* **1977**, *B16*, 4794.
(28) Kobayashi, H.; Maeda, Y.; Yanagawa, Y. *Bull. Chem. Soc. Jpn.* **1970**, *43*, 2342–2346.
(29) Lang, G.; Spartalian, K.; Reed, C. A.; Collman, J. P. *J. Chem. Phys.* **1978**, *69*, 5424–5427.
(30) Strauss, S. H.; Silver, M. E.; Long, K. M.; Thompson, R. G.; Hudgens, R. A.; Spartalian, K.; Ibers, J. A. *J. Am. Chem. Soc.* **1985**, *107*, 4207–4215.
(31) Zerner, M. C.; Gouterman, M.; Kobayashi, H. *Theor. Chim. Acta* **1966**, *6*, 363–400.